Entropy aided K-t Group Sparse SENSE method for highly accelerated dynamic MRI

M. Usman[1], C. Prieto[1], T. Schaeffter[1], and P. G. Batchelor[1]

[1]Division of Imaging Sciences and Biomedical Engineering, King's College London, London, United Kingdom

INTRODUCTION: Over the last few years, the combination of Compressed sensing (CS) and parallel imaging have been of great interest to accelerate MRI. For dynamic MRI, K-t sparse SENSE (K-t SS) has been proposed [1] for combining the CS based K-t Sparse method [2] with SENSE. Recently, K-t group sparse method (K-t GS) [3] has been shown to outperform K-t Sparse for single coil reconstruction, by exploiting the sparsity and the structure within the sparse representation (x-f space) of dynamic MRI. In this work, we propose to extend K-t GS to parallel imaging acquisition in order to achieve higher acceleration factors by exploiting the spatial sensitive encoding from multiple coils. This approach has been called K-t group Sparse SENSE (K-t GSS). In contrast with the previous single-coil based K-t GS method for which a performance parameter is manually optimized for every frequency encode; we propose an entropy based scheme for *automatic* selection of this parameter. Results from retrospectively undersampled cardiac gated data show that K-t GSS outperformed K-t sparse SENSE at high acceleration factors (up to 16 fold).

THEORY: Let **X** be the signal in x-f space whose elements $\mathbf{X_i}$ {i=1, 2,.., N} are assigned to K distinct groups $\{g_1,g_2,..,g_K\}$ which are non overlapping and whose union gives the signal **X**. K-t GS formulation is given as: $\min_X\|\mathbf{X^g}\|_{1,2}$ subject to $\|\mathbf{AX} - \mathbf{b}\|_2 \le \sigma$ **(1),** where $\|\mathbf{X^g}\|_{1,2}$ is the mixed l_1-l_2 norm given as $\|\mathbf{X^g}\|_{1,2} = \|\mathbf{X^g}_1\|_2+\|\mathbf{X^g}_2\|_2+.......+\|\mathbf{X^g}_K\|_2$, $\|\mathbf{X^g}_j\|_2$ being the l_2 norm of the vector containing all elements in x-f space assigned to the group $\{g_j\}$, **A** is the encoding matrix comprising the inverse Fourier transform along temporal dimension, Fourier transform along spatial dimension and the undersampling operator, **b** is the set of measurements in k-t space and σ is a parameter that controls the fidelity of the reconstruction to the measured data. By extending the K-t GS method to parallel MRI, instead of performing reconstruction for each coil separately, the multicoil SENSE model given by concatenation of the individual models is solved. Let L be the number of coils, the K-t GSS formulation is given by: $\min_X\|\mathbf{X^g}\|_{1,2}$ subject to $\|\mathbf{EX} - \mathbf{B}\|_2 \le \sigma$ **(2),** where the encoding matrix **E** now also includes the coil sensitivities $\mathbf{C_i}$'s, thus $\mathbf{E=[AC_1\ AC_2 ...\ AC_L]}$; and **B** comprises M measurements each from L coils given as $\mathbf{B=[b_1\ b_2 ...\ b_L]}$.

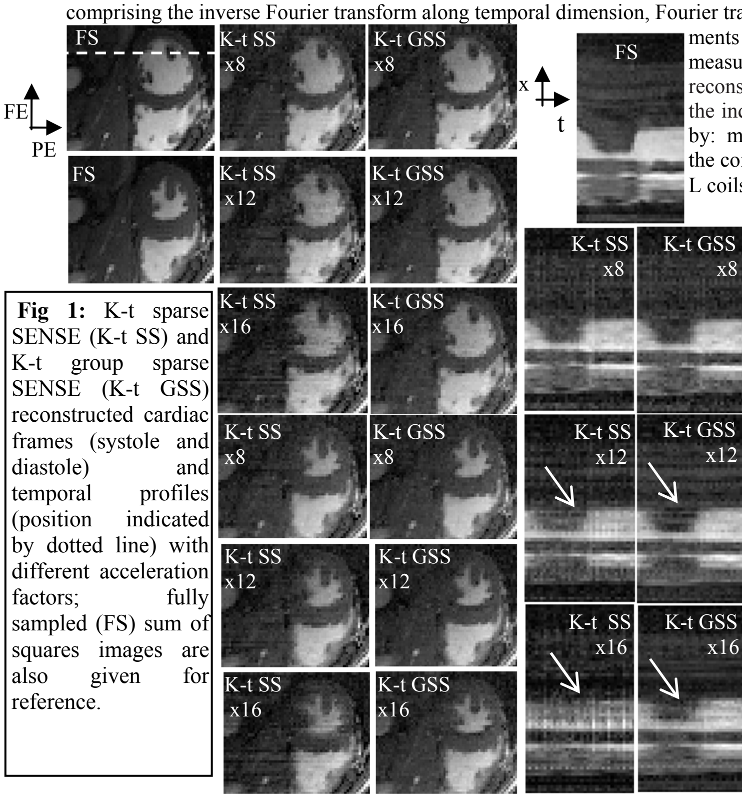

Fig 1: K-t sparse SENSE (K-t SS) and K-t group sparse SENSE (K-t GSS) reconstructed cardiac frames (systole and diastole) and temporal profiles (position indicated by dotted line) with different acceleration factors; fully sampled (FS) sum of squares images are also given for reference.

METHOD: K-t GSS method comprises three steps (1) support estimation (2) group assignment and (3) signal recovery. For support estimation, a low resolution training scan is used to identify the support region in the x-f space. After zero-padded sum of squares (SOS) reconstruction of the multiple-coil low resolution images, a threshold is set above the noise level in the corresponding x-f space. The x-f space elements having intensities above the threshold constitute the support region. In the group assignment step, run-length encoding (RLE) scheme [4] is used to form groups from support region; elements in the x-f space that are not part of the support are each assigned as an individual group. Once the group assignment is done, the signal recovery is performed via K-t GSS formulation in Eq (2). For support estimation in the single-coil K-t GS method, the threshold above the noise level is manually tuned for every frequency encode to obtain the optimal reconstruction performance. Here, we propose a retrospective entropy based *automatic* threshold selection procedure. Starting from a minimum threshold equal to the noise level in the SOS training x-f space, the threshold is increased in small increments of size ΔT. K-t GSS reconstruction is performed using support estimated from each threshold setting, with entropy H(x-f) computed for the reconstructed x-f space. The threshold level for which the entropy H(x-f) stops decreasing and gets saturated is selected to be the optimal threshold.

EXPERIMENT: A fully sampled retrospective cardiac gated CINE SSFP sequence was performed on a Philips 1.5T Achieva system in a healthy volunteer. The scan parameters were: FOV: 320x320 mm^2, TE/TR: 1.4/3.3 ms, acquisition matrix size: 160x156, 40 cardiac phases, 5 channel cardiac coil. A separate training scan was performed for the estimation of support in x-f space. Training data was composed of 20 fully sampled central k-space lines (approximately 12.5% of fully sampled k-space data). The acquired data was simulated by retrospectively under-sampling the fully sampled data in k-t space with uniform random pattern for each coil. K-t SS and K-t GSS reconstructions were done with acceleration factors up to 16. The reconstructions were implemented in MATLAB using spectral projected gradient (SPG) based reconstruction solver [5].

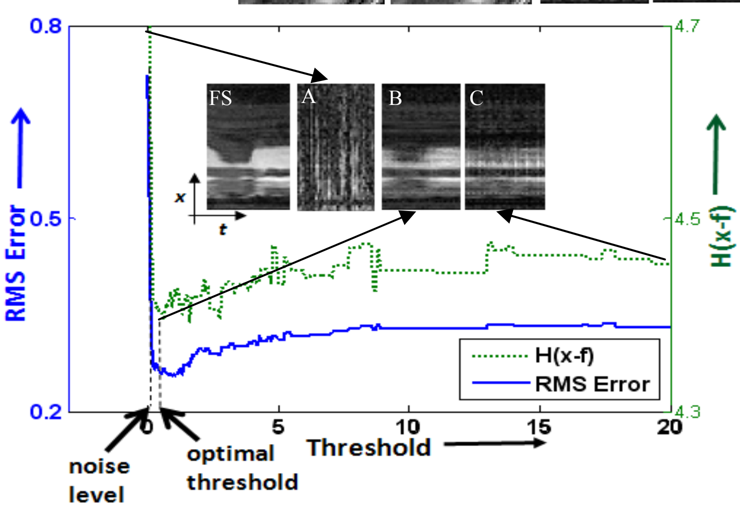

Fig. 2: For K-t GSS reconstruction (16 fold acceleration), behavior of the relative RMS reconstruction error and entropy of reconstructed x-f space H(x-f) as a function of different support estimation thresholds set in SOS (sum of squares) training x-f space. K-t GSS reconstructed temporal profiles (labeled A, B and C) at selected threshold levels are also shown, fully sampled (FS) profile is also given for reference.

RESULTS and DISCUSSION: Reconstructed images for two different frames (systole and diastole) are shown in Fig.1 for K-t SS and K-t GSS methods with different reduction factors. Temporal profiles are also included in Fig.1. At very high reduction factors (16-fold acceleration), K-t SS method exhibited noisy reconstructions with significant residual artifacts and temporal blurring, whilst K-t GSS eliminates most of the artifacts introducing less temporal blurring (see region of interest pointed by arrows in Fig.1). For a specific temporal profile reconstructed with K-t GSS method for 16-fold acceleration, Fig.2 shows the plots of relative root mean square (RMS) error of the reconstruction and the entropy of reconstructed x-f space H(x-f) as a function of threshold set in SOS training x-f space. The reconstructed temporal profiles at selected thresholds are also shown. Both H(x-f) and RMS error had similar variations (87.4% cross correlation) as a function of threshold settings in the SOS training x-f space. For the optimal threshold setting, the reconstructed x-f space was less noisy and had a better definition of object features (see reconstructed profile labeled B in Fig 2). This resulted in low values of both the reconstruction error and H(x-f). For a threshold setting higher or lower than the optimal level, the reconstructions exhibited noisy artifacts resulting in higher values of entropy and RMS error (see reconstructed profiles labeled A and C in Fig. 2). Hence, H(x-f) gave a good *a priori* predictor of *a posteriori* reconstruction quality and RMS reconstruction error. In the limiting case where the threshold is set below the minimum value in the SOS training x-f space, the K-t GSS formulation in Eq (2) is reduced to minimum l_2 norm reconstruction. On the other hand, for a threshold set above the maximum value in the SOS training x-f space, the reconstruction formulation is reduced to K-t SS formulation in Eq (1).

CONCLUSION: By exploiting the sparsity, the structure within sparse representation and information from multiple coils, our method was able to achieve reconstructions with better spatial and temporal quality compared to the existing standard methods in dynamic MRI.

REFERENCES: [1] Otazo et al, MRM 2010, [2] Lustig et al, ISMRM 2006 [3] Usman at al, ISMRM 2010 [4] Haralik et al, Computer and Robot vision, 1992 [5] Van den Berg et al, SIAM 2008.